

Enzymatically active biomimetic micropropellers for the penetration of mucin gels

Debora Walker,^{1,2} Benjamin T. Käsdorf,³ Hyeon-Ho Jeong,¹ Oliver Lieleg,³ Peer Fischer^{1,2*}

2015 © The Authors, some rights reserved; exclusive licensee American Association for the Advancement of Science. Distributed under a Creative Commons Attribution NonCommercial License 4.0 (CC BY-NC). 10.1126/sciadv.1500501

In the body, mucus provides an important defense mechanism by limiting the penetration of pathogens. It is therefore also a major obstacle for the efficient delivery of particle-based drug carriers. The acidic stomach lining in particular is difficult to overcome because mucin glycoproteins form viscoelastic gels under acidic conditions. The bacterium *Helicobacter pylori* has developed a strategy to overcome the mucus barrier by producing the enzyme urease, which locally raises the pH and consequently liquefies the mucus. This allows the bacteria to swim through mucus and to reach the epithelial surface. We present an artificial system of reactive magnetic micropropellers that mimic this strategy to move through gastric mucin gels by making use of surface-immobilized urease. The results demonstrate the validity of this biomimetic approach to penetrate biological gels, and show that externally propelled microstructures can actively and reversibly manipulate the physical state of their surroundings, suggesting that such particles could potentially penetrate native mucus.

INTRODUCTION

The human body has numerous mechanisms that protect it against the invasion of pathogens. These defenses include mucosal layers that line all wet epithelial surfaces, including the airway system and lungs, the gastrointestinal tract, and the urogenital tract. Mucus barriers not only make it difficult for microorganisms to reach and penetrate the host's tissues but also hinder the delivery of other substances such as potential pharmaceutical carriers, while allowing nutrients and other beneficial substances to pass freely (1–3). The stomach poses a particular challenge in this context, because here the combination of the mucus layer and the very low pH presents a major obstacle for various drug delivery applications (4, 5). At the same time, most pharmaceuticals on the market are designed for oral administration (5); hence, efficient approaches for drug uptake in the gastrointestinal tract are of significant medical importance.

The glycoprotein mucin, a major component of mucus, is primarily responsible for the medium's mechanical properties. Mucin forms a highly viscoelastic interconnected network that regulates transport at the gastric epithelial surface. The complex filtering behavior can be traced back to two main effects, namely, the structure and pore size of the polymeric network, as well as mucin-particle interactions (1, 3, 5–7). Previous studies have verified that penetration of mucin gels may be enhanced by the addition of mucolytic agents (8–11), and it has been shown that the presence of degrading enzymes in the medium can enhance the transport of particles in other hydrogels as well (12). However, complete degradation of the mucus is generally not desirable because of the gel's important protective function and the resulting need to preserve the integrity of the mucosa (5). Many pathogens have developed strategies to overcome the mucus barrier, which include specific surface interactions, a modulation of mucin production, and the use of mucolytic enzymes; these approaches have been suggested to be potentially transferrable to artificial particulate delivery systems (13–16). *Helicobacter pylori*, a flagellated bacterium that inhabits the stomach and is associated with peptic ulcer disease and gastritis (17, 18), uses a simple

approach to locally and reversibly manipulate the gastric mucus. It has recently been demonstrated that *H. pylori* secretes large amounts of the enzyme urease not only as a defense against the harsh acidic environment of the stomach but also to actively change mucus viscosity and facilitate propulsion, as shown schematically in Fig. 1 (19). Urease catalyzes the hydrolysis of urea, which results in the release of ammonia. The subsequent local rise in pH induces a gel-sol transition of the mucus and thus reduces its viscosity by liquefying it (4, 20). It could be shown that *H. pylori* bacteria are capable of moving freely through mucin solutions at neutral pH, whereas they are immobile in acidic mucin gels if the solution does not contain urea, even though they can be observed to move their flagella under these conditions (19). If urea is added to the solution under acidic conditions, the bacteria again move almost freely.

Here, we demonstrate an artificial system of magnetic micropropellers that mimic *H. pylori* in their strategy to propel through gastric mucus (see Fig. 1). Thus far, drug carriers and other particles have been treated mostly with substances that modulate mucus-surface interactions, such as polyethylene glycol, various polymers, adsorbed bile salts, lectins, and microbial ligands (7, 16, 21–24). The present study shows that it is possible to significantly enhance the mobility of microparticles in mucin gels by urease immobilization on their surface. This avoids both a systemic treatment and the use of enzymes that irreversibly degrade the protective mucus lining. To implement *H. pylori*'s strategy for active mucin penetration described above, we developed magnetic micropropellers that are stable under acidic conditions, are capable of efficient propulsion in mucin solutions at neutral pH, and have a high enough activity of immobilized urease on the surface to allow for propulsion in slightly acidified mucin gels that contain urea. The results demonstrate the validity of using this catalytic approach to penetrate viscoelastic biological media. To our knowledge, this is the first example of an externally propelled microstructure that actively manipulates the physical state of its surroundings by changing the rheological properties of the medium.

Several kinds of artificial micro- and nanostructures that can be wirelessly moved at low Reynolds number have been developed in recent years (25–33). It has been shown that magnetic helical (screw-like) structures can be actuated precisely, even over larger distances, when they are subjected to a homogeneous rotating magnetic field (25, 26, 33–35). Most studies have shown propulsion in low-viscosity model fluids, such

¹Max Planck Institute for Intelligent Systems, Heisenbergstrasse 3, 70569 Stuttgart, Germany.

²Institute for Physical Chemistry, University of Stuttgart, Pfaffenwaldring 55, 70569 Stuttgart, Germany.

³Institute for Medical Engineering and Department of Mechanical Engineering, Technische Universität München, Boltzmannstrasse 11, 85748 Garching, Germany.

*Corresponding author. E-mail: fischer@is.mpg.de

as water, simple buffer solutions, serum, or blood (25, 26, 31, 34). Recently, the retention of Zn-powered micromotors in the stomach was demonstrated to be higher than that of passive particles (36). It was furthermore shown that the ability of helical propellers to move through macromolecular networks of hyaluronic acid depends strongly on the size of the penetrating particle, and that particles with diameters on the order of the medium's pore size can penetrate these biological gels much more effectively than larger particles (33). A different strategy to overcome viscous tissues or penetrate a protective mucous lining is to render these particles reactive. Here, we borrow such a mechanism of active micropropulsion from nature and mimic the mucus penetration strategy of *H. pylori*.

RESULTS

Fabrication of acid-stable micropropellers

The micropropellers used in this study are produced via a highly parallel physical vapor deposition (PVD) process, known as glancing angle deposition (GLAD) (37, 38). We generated glass (SiO_2) helices into which a thin magnetic section was incorporated. The entire fabrication process of the enzyme-functionalized magnetic propellers is depicted in Fig. 2. Details of the fabrication process have been reported previously (39). However, here, the magnetic Ni section was deposited on the structures at the very end of the PVD process, and the GLAD step was then followed by atomic layer deposition (ALD) where the helices were coated with an 8-nm shell of alumina (Al_2O_3) to render the magnetic section resistant to oxidation in acidic solution (this was verified by propulsion experiments after dispersing the particles in pH 4.6 phosphate buffer for 24 hours). The micropropellers are shaped like small screw-like drills that are magnetized orthogonal to the helix axis; thus, when a rotating magnetic field is applied, the propellers rotate about their long axis and thus translate by virtue of their chiral shape (25, 39, 40).

Urease immobilization

We found that the ALD-stabilized micropropellers could be readily functionalized with urease, using published protocols (41, 42). For this, the propellers were first treated with 3-aminopropyltriethoxysilane (APTES) and activated with glutaraldehyde (GA), which then allowed the enzyme to be coupled to the surface. A visual control of the pH

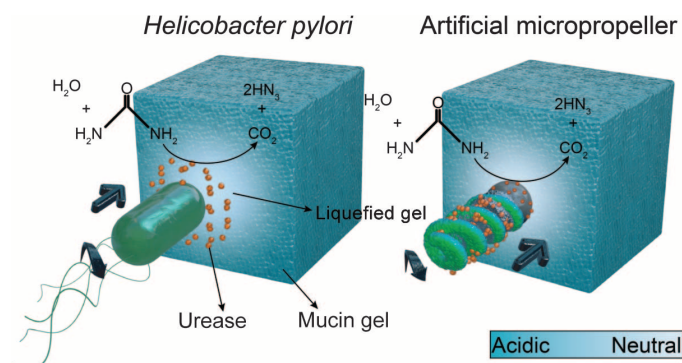


Fig. 1. Mechanism for mucin penetration. Schematic illustration of the propulsion strategy of *H. pylori* through mucin gels and the catalytically active magnetic micropropellers presented here. The enzyme on the helices' surface hydrolyzes urea and liquefies the environment via the resulting local rise in pH.

increasing ability of urease-functionalized control particles is shown in Fig. 3 to ensure that this coupling procedure maintains the enzymatic activity of the urease. Silica beads with a diameter of $\sim 50 \mu\text{m}$ were functionalized in the same manner as the micropropellers and were added into a solution of urea together with a small amount of the pH indicator bromothymol blue. The color change over the course of several minutes clearly visualizes the local increase in pH. The enzyme activity (maximum rate at high urea concentrations) of urease immobilized on silica particles (diameter, $1.5 \mu\text{m}$) was furthermore quantified using an established method (43). The results were generally on the order of $\sim 1 \mu\text{mol s}^{-1}$ urea hydrolysis per gram of silica particles. Stöber particles are smooth and have a specific surface area not much higher than their geometric surface area (44, 45); thus, this value translates very roughly to an ammonia release rate on the order of $\sim 1 \mu\text{mol s}^{-1} \text{m}^{-2}$. Using Fick's first law and an ion diffusion coefficient of $\sim 5 \times 10^{-11} \text{m}^2 \text{s}^{-1}$ in mucus (46), one can estimate that the Stöber particles would be able to maintain a concentration difference on their surface relative to the medium on the order of $\sim 20 \mu\text{M}$. Taking into account that silica GLAD structures are rough/porous with specific surface areas on the order of hundreds of square meters per gram (47), this yields a concentration difference on the order of $\sim 1 \text{mM}$ on the surface of the micropropellers. This value is in agreement with the observation that propulsion experiments were only successful at HCl concentrations less than 1mM above the minimum amount needed for gelation (see below).

After functionalization with urease, the micropropellers (Fig. 2) were magnetized on the wafer. Dispersion in the desired solution by sonication allowed individual structures to be propelled by a weak rotating homogeneous magnetic field of about 10mT (100G).

Mucin gel characterization

In the stomach, *H. pylori* encounters a viscoelastic mucus gel at acidic pH. Here, we used a reconstituted system of purified porcine gastric mucins (PGMs). The addition of 5.5mM HCl to 2% PGM was chosen for subsequent propulsion experiments, because this concentration

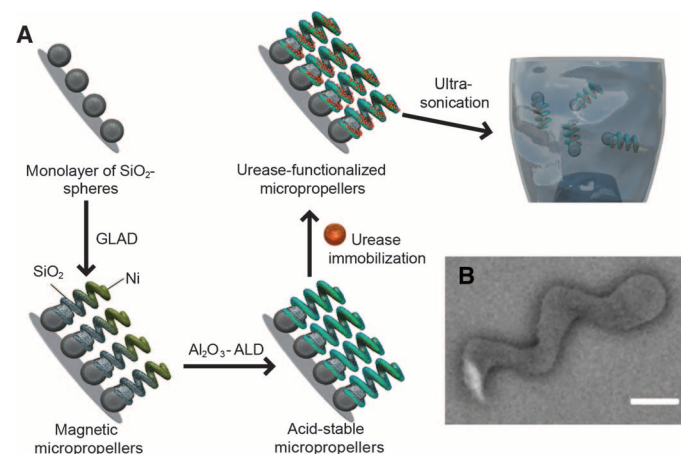


Fig. 2. Acid-stable enzyme-functionalized micropropellers. (A) Fabrication process of acid-stable enzyme-functionalized magnetic micropropellers consisting of GLAD on top of a monolayer of silica beads, atomic layer deposition (ALD) to protect the resulting magnetic helices, enzyme immobilization, and ultrasonication in solution to remove the particles from the wafer. (B) ESB-SEM (energy-selective backscatter-scanning electron microscopy) image of a magnetic micropropeller, with the Ni section clearly visible. Scale bar, 500nm .

supplied the necessary acidity for gelation. Such an HCl concentration usually led to the formation of gels with a pH between 4 and 5. The rheological measurements presented in Fig. 4A demonstrate that a 2% solution of PGMs exhibits a sol-gel transition somewhere between pH 4.5 and pH 7; that is, it behaves as a viscoelastic fluid under neutral conditions and as a viscoelastic gel at pH 4.5 [the storage modulus $G'(f)$ exceeds the loss modulus $G''(f)$ at low pH for all frequencies tested, and vice versa at neutral pH]. However, the detailed gelation transition depends on both the mucin concentration and the ionic strength of the mucin reconstitution buffer (4). We verified, therefore, that neither the use of HCl, instead of the reconstitution buffer used for the characterization of the gelation behavior, nor the addition of bile salts and urea suppressed gel formation. In addition, by sonicating a gel sample for 5 min before rheological characterization, we confirmed that ultrasonication did not have any long-term influence on the gel properties. Results of the above tests are shown in Fig. 4B.

Propulsion in mucin gels

In the following, we describe in detail how the urease-covered microparticles are able to effectively move through a mucin gel. In brief, this is achieved by two steps: First, the presence of naturally occurring bile salts prevents adhesion of the mucin to the particles' surface. Second, urea, which is also present in the stomach at concentrations of a few millimolar

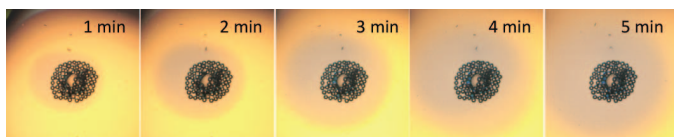


Fig. 3. Urease activity. SiO_2 beads ($\sim 50 \mu\text{m}$ in diameter) functionalized with urease using GA coupling, in a solution of 100 mM urea colored with the pH indicator bromothymol blue. The beads were dried on a coverslip and micrographs were recorded 1, 2, 3, 4, and 5 min after the addition of urea solution. The blue coloring clearly demonstrates the increase in pH due to catalytic urea hydrolysis.

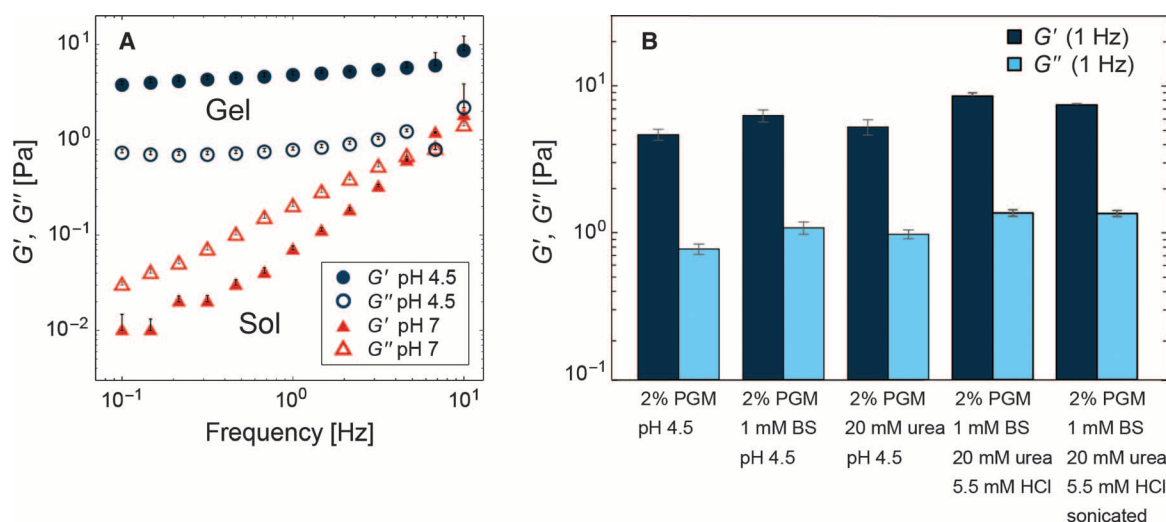


Fig. 4. Mucin rheology. (A) Viscoelastic properties of reconstituted PGMs at different pH conditions. A 2% solution of PGMs exhibits a clear sol-gel transition between pH 4.5 and pH 7. Closed symbols denote the storage modulus $G'(f)$, and open symbols denote the loss modulus $G''(f)$. (B) Gelation of the PGM solution is neither suppressed by the addition of 1 mM bile salts (BS; sodium glycodeoxycholate and sodium taurocholate) nor suppressed by the addition of 20 mM urea, the use of 5.5 mM HCl instead of a pH 4.5 reconstitution buffer, or ultrasonication.

(48–50), is converted by the urease to ammonia, which raises the pH and thus induces the gel-sol transition, thereby lowering the viscosity around the micropellers.

When placed in pure PGM solution at neutral pH (corresponding to a low viscosity), most of the time, the magnetic propellers appear to rotate when a rotating magnetic field is applied but do not exhibit any forward propulsion, even at very low concentrations of only 0.25% PGM. We postulate that this is due to mucoadhesion (1, 22, 23), that is, the adsorption of mucin to the surface of the particles. One explanation for the low motility is that adsorbed mucin reduces the rotation rate by immobilizing the particles in the polymeric matrix. However, our evidence seems to suggest that rather than exhibiting diminished rotation, the propellers become entangled in the polymer chains during rotation, which reduces their effective geometric helicity and thus their rotation-translation coupling, preventing directional movement. This explanation is supported by the tendency of the propellers to form linear chains in the direction of propulsion along which individual particles are not in direct contact but still seem rigidly connected. A video of micropellers being actuated at a frequency of 30 Hz and a magnetic field strength of 10 mT in 0.5% neutral mucin solution, together with a video of a chain of the kind mentioned above (in 0.25% mucin), can be found in the Supplementary Materials (movie S1).

Various coatings and surface passivation techniques have been designed to reduce mucoadhesion (7, 21–23). The one that proved most effective in our case, partly because it does not require any covalent surface functionalization and is thus compatible with enzyme immobilization on the surface of the micropellers, was the addition of bile salts to the mucin solutions (22). We stress that bile salts are in any case present in naturally occurring mucus of the stomach at low concentrations (51). For all experiments, we used the same combination of bile salts (that is, sodium glycodeoxycholate and sodium taurocholate) that Macierzanka *et al.* found to be optimal for preventing mucoadhesion on both latex microparticles and model food emulsion droplets (22). We found that a bile salt concentration of 1 mM was sufficient to suppress adsorption, while not interfering with the gelation ability of

the mucin solution (see Fig. 3). In neutral mucin solutions with concentrations up to 2% containing 1 mM bile salts, the micropropellers were then indeed able to propel, although both the dimensionless velocity (the velocity normalized by the helix's pitch and the frequency of the magnetic field, about 0.11 ± 0.03 at a frequency of 30 Hz and a mucin concentration of 2%) and the step-out frequency (<60 Hz at 10 mT and 2%) were lower than what can generally be observed in water or other low-viscosity Newtonian fluids (33, 39). The lower step-out frequency is plausible because of the higher viscosity of mucin relative to water, whereas the lower dimensionless velocity is potentially more surprising because some studies in other complex viscous and viscoelastic environments have found propulsion enhancement relative to low-viscosity Newtonian fluids (33, 52–54). However, theoretically, both enhancement and reduction of propulsion velocities in viscoelastic media compared to Newtonian liquids have been predicted, depending on the exact conditions, particle geometry, and fluid model (55–60).

Next, we verified that the micropropellers are unable to move at acidic pH where the mucins form a viscoelastic gel. In solutions of 2% mucin, 1 mM bile salts, and small amounts of hydrochloric acid (for our samples, this value was typically slightly more than 5 mM, but it can vary between different mucin batches), no propulsion could be observed at a magnetic field strength of 10 mT. The gel state of the mucin was obvious in that it not only prevented propulsion of the magnetic helices but also reduced Brownian motion of any passive particles in the sample. Adding 20 mM urea to the solution did not change this observation in the case of unfunctionalized propellers, which is consistent with our finding that this amount of urea does not interfere with the gelation properties of a 2% solution of PGMs (see Fig. 3).

Finally, we tested whether micropropellers functionalized with urease are indeed able to navigate through a mucin gel by actively changing the rheological properties of its surroundings. We observed effective propulsion of urease-functionalized micropropellers in urea-containing mucin solutions containing 5.5 mM HCl. Figure 5B shows tracks of helices with immobilized urease in such slightly acidified mucin solutions, and the propellers' average velocity obtained under these conditions is shown in Fig. 5E. In the absence of urease, these micro-

propellers do not move (see Fig. 5A), as expected. The corresponding videos can be found in the Supplementary Materials. It should be noted that the velocity observed for the micropropellers that induce a gel-sol transition is lower than what can be observed for micropropellers moving in low-viscosity mucin control solutions (that is, at neutral pH). At a frequency of 30 Hz and a magnetic field strength of 10 mT, the propellers in the neutral control mucin solution moved at an average speed of $2.6 \pm 0.8 \mu\text{m s}^{-1}$, whereas the catalytic propellers in the acidified mucin were observed to move at an average speed of $1.4 \pm 0.5 \mu\text{m s}^{-1}$. Our experiments clearly demonstrate that only the urease-functionalized micropropellers can actively penetrate the mucin gel and that this active motion is only enabled in the presence of the enzyme substrate urea.

DISCUSSION

The concentrations used in our mucus model differ only in a few respects from those found in the actual mucosal stomach lining. The mucin content, which is one of the most crucial parameters that determine the viscoelasticity of the material, is on the lower end of the range typically encountered in the gastric mucus layer, where one typically finds concentrations of 2 to 5% mucin by weight (2, 6). Typical urea concentrations in the human stomach are on the order of several millimolar in healthy subjects and can be higher for a number of pathological conditions (48–50, 61); therefore, the concentration used in this study is biomedically relevant. The same holds true for the concentration of bile salts used here (1 mM), because the bile acid content in the gastric juice can reach hundreds of micromolar in healthy subjects (51). However, the HCl content can exceed 100 mM in the stomach (62), which is significantly more than the amount that was used in this study. One of the reasons for this is that the commercially available urease (isolated from jack bean) is not optimized for and thus not very active at low pH. So-called acid ureases (63) could potentially provide significantly higher enzyme activity under conditions found in the stomach and should be used in potential applications; however, these enzymes were not available to the authors for this study. Furthermore, future

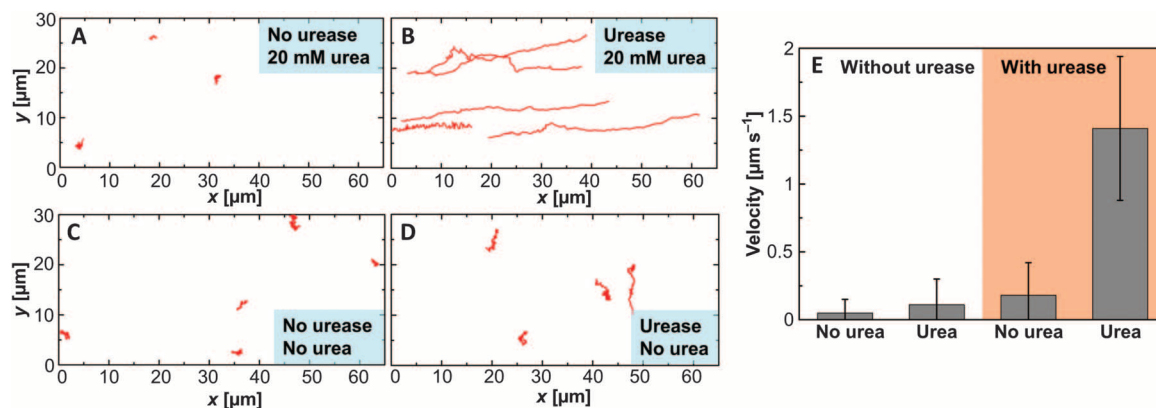


Fig. 5. Propulsion in mucin gels. (A to D) Tracks of micropropellers with (B and D) and without (A and C) urease immobilized on the surface, in an acidified 2% mucin gel with (A and B) and without (C and D) 20 mM urea over a time frame of 25 s. The particles were propelled in the x direction at a frequency of 30 Hz and a magnetic field strength of 10 mT. Each graph shows the tracks from one video recording. (E) The average velocity under these conditions is shown and represents an average of a minimum of 50 particles tracked over at least 10 s. Only the x component of the velocity was taken into account; the small drift in the y direction that can sometimes be observed when the particles are close to the glass surface [as in (D)], or “kinks” in the y direction due to hydrodynamic interactions with another propeller in proximity [as in the topmost trajectory in (B)], was neglected. The corresponding videos can be found in the Supplementary Materials.

reactive microparticle systems could be even more effective if the overall enzyme loading is increased; that is, urease is not immobilized on the surface but instead carried in larger amounts in the bulk volume of the particle, so that the enzymes can more quickly neutralize higher amounts of acid, thus allowing for more efficient forward propulsion. This could be achieved if, for instance, porous materials are used for the basis of the microparticles or by immobilizing larger amounts of enzyme onto the particle surface, for example, via branched polymer linkers or enzyme cross-linking.

In summary, our experiments demonstrate that it is possible to engineer microparticles in such a way that they actively manipulate their environment and thus become mobile. We verified that strategies for the penetration of complex biological hydrogel barriers, which are specifically designed to hinder the transport of micrometer-sized structures (that is, certain pathogens), can be borrowed from microorganisms. Magnetically actuated micropropellers can successfully navigate through mucin gels when functionalized with urease, which allows them to induce a gel-sol transition in the surrounding biopolymer network. This mimics the molecular strategy by which the bacterium *H. pylori* achieves motility in the mucus lining of the stomach. In addition to being of interest for the further development of remotely steerable “microbots,” our results are also relevant for the generation of more efficient drug and/or particle delivery systems. In particular, our study suggests that uptake and delivery across mucosal barriers, for instance, in the gastrointestinal tract, can potentially be improved even for passively diffusing drug carriers, if they are functionalized to reversibly reduce the viscoelastic properties of the mucosa.

MATERIALS AND METHODS

Micropropeller fabrication

The magnetic micropropellers were produced using a previously described method (39), with the magnetic section at one end of the helix. A Langmuir-Blodgett monolayer of 500-nm silica beads was used as a seed layer. After the GLAD step, a thin alumina (Al_2O_3) layer was grown to cover the helices' surface using ALD (Savannah 100, Cambridge NanoTech) at $T = 100^\circ\text{C}$ with a growth rate of 0.1 nm per cycle by repeatedly injecting trimethylaluminum for 0.15 s and deionized water for 0.15 s. The stabilized micropropellers were magnetized in plane (that is, transversally relative to the individual helix) at 1.8 T in an electromagnet.

Enzyme immobilization

For the urease immobilization, the wafer with micropropellers (or a few milligrams of silica beads for the control experiments) was first immersed in a 2 volume % solution of APTES (Sigma-Aldrich) and ~0.2 M ammonium hydroxide in ethanol at room temperature for 1.5 hours. After rinsing with ethanol and water, the sample was then immersed in an aqueous solution of 2.5% glutaraldehyde in 50 mM phosphate buffer (pH 7) containing sodium cyanoborohydride (~1 mg/ml) at room temperature for 3 hours. After thoroughly rinsing with water, the wafer was then suspended in 50 mM phosphate buffer (pH 7) again containing sodium cyanoborohydride (~1 mg/ml) and urease (~2 mg/ml; type IX from jack bean, Sigma-Aldrich) at 4°C overnight. The sample was then washed with 25 mM phosphate buffer (pH 7) and stored on the wafer at 4°C . Enzyme-functionalized samples were generally used in the experiments for about 2 weeks before a fresh sample was

prepared. The enzyme activity of functionalized silica beads was confirmed quantitatively according to the following procedure: 0.5 mg of functionalized silica particles (1.5 μm) was incubated at room temperature in 250 μl of a solution of 50 mM urea and 40 mM NaCl for 5 to 30 min. The reaction was quenched by the addition of 550 μl of a solution of 60 mM sodium salicylate (Sigma-Aldrich) and 5 mM sodium nitroprusside (Sigma-Aldrich) and 400 μl of 10 mM sodium hypochlorite in 400 mM sodium hydroxide solution. After centrifugation and incubation at room temperature for roughly 30 min, the absorbance of the solution at 690 nm was determined with a Cary 4000 UV-Vis Spectrometer. Calibration was performed using solutions containing appropriate amounts of ammonium sulfate. The supernatant of the functionalized particles after washing was verified to exhibit negligible enzyme activity. Washing of the particles involved multiple redispersion steps using ultrasonication, which did not result in a measurable change in enzyme activity of the particles or of the supernatant.

Mucin preparation and characterization

Porcine gastric mucins were purified from scrapings of fresh pig stomachs essentially as described previously (64), with the exception that the cesium chloride density gradient ultracentrifugation was omitted. In brief, mucus was collected from the surface of pig stomachs by gentle scraping and dissolved in phosphate-buffered saline (10 mM, 170 mM NaCl adjusted to pH 7.4). The mucins were then purified by a series of centrifugation and size-exclusion chromatography steps and then concentrated and desalted by cross-flow dialysis until a conductance of less than 50 μS was reached. Then, the obtained mucin MUC5AC was stored in lyophilized form at -80°C until further use. Such lyophilized mucins can be reconstituted at a given pH and ionic strength by rehydration at 4°C overnight. Reconstituted mucin solutions exhibit a pH-dependent sol-gel transition as described previously, provided that the ionic strength of the rehydration buffer is kept low (64).

Rheological characterization of mucin solutions and gels was performed on a stress-controlled shear rheometer (MCR 302, Anton Paar) using a plate/plate measuring setup (PP25, Anton Paar) and 150- μm plate separation. When determining frequency-dependent viscoelastic moduli, small torques in the range of 0.5 μNm were applied to ensure a linear material response. Phosphate-buffered saline (10 mM, pH 7.0) and acetate buffer (10 mM, pH 4.5) were used as reconstitution buffers.

Propulsion experiments

For the propulsion experiments, solutions of 4% mucin containing 1 mM sodium taurocholate and 1 mM sodium glycodeoxycholate (Sigma-Aldrich) were prepared at 4°C overnight. As-prepared solutions were used in experiments within 24 hours of reconstitution. This solution was then mixed thoroughly 1:1 with a solution containing the appropriate amount of hydrochloric acid (11 mM for the acidified gels and 0 mM for the control experiments) and urea (0 or 40 mM). Right before the propulsion experiments, the micropropellers were dispersed in the solution by ultrasonication. The mixture was then transferred to a 25- μl gene frame (Thermo Scientific) and positioned in a water-cooled three-axis Helmholtz coil setup described previously (39). Propulsion experiments were performed at room temperature within 5 to 20 min of propeller dispersion at a magnetic field strength of 10 mT. Videos were recorded with a minimum pixel resolution of 5 pixels/ μm . For the velocity measurements, the particles were tracked for a minimum of 10 s and the average velocity over that time frame only in the direction of propulsion

was determined. The reported results therefore do not reflect the amount of Brownian motion present in the sample or any motion perpendicular to the axis of rotation, which can arise from interactions with the surface of the coverslip (that is, rolling). For each reported value, at least 50 particles were averaged. The propulsion experiments with enzymatically active and plain propellers in urea-containing mucin gels were repeated and reproduced from scratch four times (one of which was performed using a different batch of lyophilized mucin and therefore needed a different acid concentration for the experiment to succeed). The control experiments without urea were each performed at least twice. Propulsion in mucin concentrations other than 2% was tested only under neutral pH. Even in the sol state, 4% mucin solutions were too viscous to allow for propulsion at the magnetic field strengths used in this study. For very low mucin concentrations, that is, below 0.5%, rheological measurements indicate that gelation does not occur any longer; hence, accordingly, an experiment involving an induced gel-sol transition would not be possible anymore.

SUPPLEMENTARY MATERIALS

Supplementary material for this article is available at <http://advances.sciencemag.org/cgi/content/full/1/11/e1500501/DC1>

Movie S1. Magnetic microhelices in neutral PGM solutions (0.5% mucin in the left panel and 0.25% in the right panel) being propelled in the *x* direction at a frequency of 30 Hz and a magnetic field strength of 10 mT.

Movie S2. Magnetic microhelices with and without urease immobilized on the surface in an acidified 2% mucin gel containing 1 mM bile salts, with and without 20 mM urea over a time frame of 40 s.

REFERENCES AND NOTES

- O. Liele, I. Vladescu, K. Ribbeck, Characterization of particle translocation through mucin hydrogels. *Biophys. J.* **98**, 1782–1789 (2010).
- S. K. Lai, Y.-Y. Wang, D. Wirtz, J. Hanes, Micro- and macrorheology of mucus. *Adv. Drug Deliv. Rev.* **61**, 86–100 (2009).
- R. A. Cone, Barrier properties of mucus. *Adv. Drug Deliv. Rev.* **61**, 75–85 (2009).
- J. P. Celli, B. S. Turner, N. H. Afdhal, R. H. Ewoldt, G. H. McKinley, R. Bansil, S. Erramilli, Rheology of gastric mucin exhibits a pH-dependent sol-gel transition. *Biomacromolecules* **8**, 1580–1586 (2007).
- L. M. Ensign, R. Cone, J. Hanes, Oral drug delivery with polymeric nanoparticles: The gastrointestinal mucus barriers. *Adv. Drug Deliv. Rev.* **64**, 557–570 (2012).
- R. Bansil, B. S. Turner, Mucin structure, aggregation, physiological functions and biomedical applications. *Curr. Opin. Colloid Interface Sci.* **11**, 164–170 (2006).
- J. Kirch, A. Schneider, B. Abou, A. Hopf, U. F. Schaefer, M. Schneider, C. Schall, C. Wagner, C.-M. Lehr, Optical tweezers reveal relationship between microstructure and nanoparticle penetration of pulmonary mucus. *Proc. Natl. Acad. Sci. U.S.A.* **109**, 18355–18360 (2012).
- J. S. Suk, S. K. Lai, N. J. Boylan, M. R. Dawson, M. P. Boyle, J. Hanes, Rapid transport of mucin-inert nanoparticles in cystic fibrosis sputum treated with *N*-acetyl cysteine. *Nanomedicine* **6**, 365–375 (2011).
- N. N. Sanders, S. C. De Smedt, E. Van Rompaey, P. Simoens, F. De Baets, J. Demeester, Cystic fibrosis sputum: A barrier to the transport of nanospheres. *Am. J. Respir. Crit. Care Med.* **162**, 1905–1911 (2000).
- S. Ferrari, C. Kitson, R. Farley, R. Steel, C. Marriott, D. A. Parkins, M. Scarpa, B. Wainwright, M. J. Evans, W. H. Colledge, D. M. Geddes, E. W. F. W. Alton, Mucus altering agents as adjuncts for nonviral gene transfer to airway epithelium. *Gene Ther.* **8**, 1380–1386 (2001).
- I. Vladescu, O. Liele, S. Jang, K. Ribbeck, An adsorption chromatography assay to probe bulk particle transport through hydrogels. *J. Pharm. Sci.* **101**, 436–442 (2012).
- J. H. Hou, A. E. Cohen, Motion induced by asymmetric enzymatic degradation of hydrogels. *Soft Matter* **8**, 4616–4624 (2012).
- A.-R. Colina, F. Aumont, N. Deslauriers, P. Belhumeur, L. de Repentigny, Evidence for degradation of gastrointestinal mucin by *Candida albicans* secretory aspartyl proteinase. *Infect. Immun.* **64**, 4514–4519 (1996).
- S. Z. Hasnain, M. A. McGuckin, R. K. Grencis, D. J. Thornton, Serine protease(s) secreted by the nematode *Trichuris muris* degrade the mucus barrier. *PLOS Negl. Trop. Dis.* **6**, e1856 (2012).
- A. J. Silva, K. Pham, J. A. Benitez, Haemagglutinin/protease expression and mucin gel penetration in El Tor biotype *Vibrio cholerae*. *Microbiology* **149**, 1883–1891 (2003).
- C. Gamazo, N. Martin-Arbella, A. Brotons, A. I. Camacho, J. M. Irache, Mimicking microbial strategies for the design of mucus-permeating nanoparticles for oral immunization. *Eur. J. Pharm. Biopharm.* **96**, 454–463 (2015).
- G. Sachs, D. L. Weeks, K. Melchers, D. R. Scott, The gastric biology of *Helicobacter pylori*. *Annu. Rev. Physiol.* **65**, 349–369 (2003).
- B. J. Marshall, J. R. Warren, G. J. Francis, S. R. Langton, C. S. Goodwin, E. D. Bincow, Rapid urease test in the management of *Campylobacter pyloridis*-associated gastritis. *Am. J. Gastroenterol.* **82**, 200–210 (1987).
- J. P. Celli, B. S. Turner, N. H. Afdhal, S. Keates, I. Ghiran, C. P. Kelly, R. H. Ewoldt, G. H. McKinley, P. So, S. Erramilli, R. Bansil, *Helicobacter pylori* moves through mucus by reducing mucin viscoelasticity. *Proc. Natl. Acad. Sci. U.S.A.* **106**, 14321–14326 (2009).
- X. Cao, R. Bansil, K. R. Bhaskar, B. S. Turner, J. T. LaMont, N. Niu, N. H. Afdhal, pH-dependent conformational change of gastric mucin leads to sol-gel transition. *Biophys. J.* **76**, 1250–1258 (1999).
- S. K. Lai, D. E. O'Hanlon, S. Harrold, S. T. Man, Y.-Y. Wang, R. Cone, J. Hanes, Rapid transport of large polymeric nanoparticles in fresh undiluted human mucus. *Proc. Natl. Acad. Sci. U.S.A.* **104**, 1482–1487 (2007).
- A. Macierzanka, N. M. Rigby, A. P. Corfield, N. Wellner, F. Böttger, E. N. C. Mills, A. R. Mackie, Adsorption of bile salts to particles allows penetration of intestinal mucus. *Soft Matter* **7**, 8077–8084 (2011).
- M. Gu, H. Yildiz, R. Carrier, G. Belfort, Discovery of low mucus adhesion surfaces. *Acta Biomater.* **9**, 5201–5207 (2013).
- Y. Cu, W. M. Saltzman, Controlled surface modification with poly(ethylene)glycol enhances diffusion of PLGA nanoparticles in human cervical mucus. *Mol. Pharm.* **6**, 173–181 (2009).
- A. Ghosh, P. Fischer, Controlled propulsion of artificial magnetic nanostructured propellers. *Nano Lett.* **9**, 2243–2245 (2009).
- P. L. Venugopalan, R. Sai, Y. Chandorkar, B. Basu, S. Shivashankar, A. Ghosh, Conformal cytocompatible ferrite coatings facilitate the realization of a nanovoyager in human blood. *Nano Lett.* **14**, 1968–1975 (2014).
- W. Gao, M. D'Agostino, V. Garcia-Gradilla, J. Orozco, J. Wang, Multi-fuel driven Janus micromotors. *Small* **9**, 467–471 (2013).
- W. Gao, A. Uygun, J. Wang, Hydrogen-bubble-propelled zinc-based microrockets in strongly acidic media. *J. Am. Chem. Soc.* **134**, 897–900 (2012).
- V. Garcia-Gradilla, J. Orozco, S. Sattayasamitsathit, F. Soto, F. Kuralay, A. Pourazary, A. Katzenberg, W. Gao, Y. Shen, J. Wang, Functionalized ultrasound-propelled magnetically guided nanomotors: Toward practical biomedical applications. *ACS Nano* **7**, 9232–9240 (2013).
- K. E. Peyer, L. Zhang, B. J. Nelson, Bio-inspired magnetic swimming microrobots for biomedical applications. *Nanoscale* **5**, 1259–1272 (2013).
- F. Qiu, L. Zhang, K. E. Peyer, M. Casarosa, A. Franco-Obregón, H. Choi, B. J. Nelson, Non-cytotoxic artificial bacterial flagella fabricated from biocompatible ORMOCOMP and iron coating. *J. Mater. Chem. B*, **2**, 357–362 (2014).
- V. Magdanz, S. Sanchez, O. G. Schmidt, Development of a sperm-flagella driven micro-robot. *Adv. Mater.* **25**, 6581–6588 (2013).
- D. Schamel, A. G. Mark, J. G. Gibbs, C. Miksch, K. I. Morozov, A. M. Leshansky, P. Fischer, Nanopropellers and their actuation in complex viscoelastic media. *ACS Nano* **8**, 8794–8801 (2014).
- W. Gao, X. Feng, A. Pei, C. R. Kane, R. Tam, C. Hennessy, J. Wang, Bioinspired helical microswimmers based on vascular plants. *Nano Lett.* **14**, 305–310 (2014).
- K. Ishiyama, M. Sendoh, K. I. Arai, Magnetic micromachines for medical applications. *J. Magn. Mater.* **242–245**, 41–46 (2002).
- W. Gao, R. Dong, S. Thamphiwatana, J. Li, W. Gao, L. Zhang, J. Wang, Artificial micromotors in the mouse's stomach: A step toward in vivo use of synthetic motors. *ACS Nano* **9**, 117–123 (2015).
- M. M. Hawkeye, M. J. Brett, Glancing angle deposition: Fabrication, properties, and applications of micro- and nanostructured thin films. *J. Vac. Sci. Technol. A* **25**, 1317–1335 (2007).
- J. G. Gibbs, A. G. Mark, T.-C. Lee, S. Eslami, D. Schamel, P. Fischer, Nanohelices by shadow growth. *Nanoscale* **6**, 9457–9466 (2014).
- D. Schamel, M. Pfeifer, J. G. Gibbs, B. Miksch, A. G. Mark, P. Fischer, Chiral colloidal molecules and observation of the propeller effect. *J. Am. Chem. Soc.* **135**, 12353–12359 (2013).
- K. I. Morozov, A. M. Leshansky, The chiral magnetic nanomotors. *Nanoscale* **6**, 1580–1588 (2014).
- B. Krajewska Ureases. II. Properties and their customizing by enzyme immobilizations: A review. *J. Mol. Catal. B Enzym.* **59**, 22–40 (2009).
- K. R. C. Reddy, A. M. Kayastha, Improved stability of urease upon coupling to alkylamine and arylamine glass and its analytical use. *J. Mol. Catal. B Enzym.* **38**, 104–112 (2006).

43. H. Verdouw, C. J. A. Van Echteld, E. M. J. Dekkers, Ammonia determination based on indophenol formation with sodium salicylate. *Water Res.* **12**, 399–402 (1978).
44. A. G. Howard, N. H. Khadry, Spray synthesis of monodisperse sub-micron spherical silica particles. *Mater. Lett.* **61**, 1951–1954 (2007).
45. M. Szekeres, J. Tóth, I. Dékány, Specific surface area of Stoeber silica determined by various experimental methods. *Langmuir* **18**, 2678–2685 (2002).
46. C. V. Nicholas, M. Desai, P. Vadgama, M. B. McDonnell, S. Lucas, pH dependence of hydrochloric acid diffusion through gastric mucus: Correlation with diffusion through a water layer using a membrane-mounted glass pH electrode. *Analyst* **116**, 463–467 (1991).
47. K. M. Krause, M. T. Taschuk, K. D. Harris, D. A. Rider, N. G. Wakefield, J. C. Sit, J. M. Buriak, M. Thommes, M. J. Brett, Surface area characterization of obliquely deposited metal oxide nanostructured thin films. *Langmuir* **26**, 4368–4376 (2010).
48. C. S. Lieber, A. Lefèvre, Ammonia as a source of gastric hypoacidity in patients with uremia. *J. Clin. Invest.* **38**, 1271–1277 (1959).
49. W. D. Neithercut, A. M. El Nujumi, K. E. L. McColl, Measurement of urea and ammonium concentrations in gastric juice. *J. Clin. Pathol.* **46**, 462–464 (1993).
50. K. Blusiewicz, G. Rydzewska, A. Rydzewski, Gastric juice ammonia and urea concentrations and their relation to gastric mucosa injury in patients maintained on chronic hemodialysis. *Rocz. Akad. Med. Białymst.* **50**, 188–192 (2005).
51. B. J. Collins, P. C. H. Watt, T. O'Reilly, R. J. McFarland, A. H. G. Love, Measurement of total bile acids in gastric juice. *J. Clin. Pathol.* **37**, 313–316 (1984).
52. R. B. Kimsey, A. Spielman, Motility of Lyme disease spirochetes in fluids as viscous as the extracellular matrix. *J. Infect. Dis.* **162**, 1205–1208 (1990).
53. W. R. Schneider, R. N. Doetsch, Effect of viscosity on bacterial motility. *J. Bacteriol.* **117**, 696–701 (1974).
54. B. Liu, T. R. Powers, K. S. Breuer, Force-free swimming of a model helical flagellum in viscoelastic fluids. *Proc. Natl. Acad. Sci. U.S.A.* **108**, 19516–19520 (2011).
55. S. E. Spagnolie, B. Liu, T. R. Powers, Locomotion of helical bodies in viscoelastic fluids: Enhanced swimming at large helical amplitudes. *Phys. Rev. Lett.* **111**, 068101 (2013).
56. T. D. Montenegro-Johnson, D. J. Smith, D. Loghin, Physics of rheologically enhanced propulsion: Different strokes in generalized stokes. *Phys. Fluids* **25**, 081903 (2013).
57. H. C. Fu, V. B. Shenoy, T. R. Powers, Low-Reynolds-number swimming in gels. *Europhys. Lett.* **91**, 24002 (2010).
58. H. C. Fu, C. W. Wolgemuth, T. R. Powers, Swimming speeds of filaments in nonlinearly viscoelastic fluids. *Phys. Fluids* **21**, 033102 (2009).
59. A. M. Leshansky, Enhanced low-Reynolds-number propulsion in heterogeneous viscous environments. *Phys. Rev.* **80**, 051911 (2009).
60. V. A. Martinez, J. Schwarz-Linek, M. Reufer, L. G. Wilson, A. N. Morozov, W. C. K. Poon, Flagellated bacterial motility in polymer solutions. *Proc. Natl. Acad. Sci. U.S.A.* **111**, 17771–17776 (2014).
61. W. D. Neithercut, P. A. Rowe, A. M. El Nujumi, S. Dahill, K. E. L. McColl, Effect of *Helicobacter pylori* infection on intragastric urea and ammonium concentrations in patients with chronic renal failure. *J. Clin. Pathol.* **46**, 544–547 (1993).
62. F. Hollander, The composition and mechanism of formation of gastric acid secretion. *Science* **110**, 57–63 (1949).
63. S. Kakimoto, H. Miyashita, Y. Sumino, S.-i. Akiyama, Properties of acid ureases from *Lactobacillus* and *Streptococcus* strains. *Agric. Biol. Chem.* **54**, 381–386 (1990).
64. J. Celli, B. Gregor, B. Turner, N. H. Afdhal, R. Bansil, S. Erramilli, Viscoelastic properties and dynamics of porcine gastric mucin. *Biomacromolecules* **6**, 1329–1333 (2005).

Acknowledgments: We thank the Department Spatz, Max Planck Institute for Intelligent Systems, for scanning electron microscopy access; the Nanostructuring Laboratory, Max Planck Institute for Solid State Research, for ALD access; and A. Posada for help with designing the figures. **Funding:** We thank the Max Planck Society for financial support. This work was in part supported by the European Research Council under the ERC Grant agreement 278213, the Deutsche Forschungsgemeinschaft (DFG) as part of the project SPP 1726 (microswimmers, FI 1966/1-1), and the Baden Württemberg Stiftung as part of the project BioMatS-10. O.L. and B.T.K. acknowledge support from the DFG through project B7 “Nanoagents in 3-dimensional bio-polymer hydrogels” in the framework of SFB1032. **Author contributions:** D.W., P.F., and O.L. proposed the experiments. D.W. fabricated the micropropellers (with the exception of the ALD step), performed enzyme immobilization, verified urease activity, and conducted the propulsion experiments. B.T.K. isolated the mucin and measured its rheological properties, and H.-H.J. performed ALD. The report was written by D.W., B.T.K., O.L., and P.F. **Competing interests:** The authors declare that they have no competing interests. **Data and materials availability:** All data needed to evaluate the conclusions in the paper are present in the paper and/or the Supplementary Materials. Additional data related to this paper may be requested from the authors.

Submitted 21 April 2015

Accepted 25 September 2015

Published 11 December 2015

10.1126/sciadv.1500501

Citation: D. Walker, B. T. Käs Dorf, H.-H. Jeong, O. Lieleg, P. Fischer, Enzymatically active biomimetic micropropellers for the penetration of mucin gels. *Sci. Adv.* **1**, e1500501 (2015).

This article is published under a Creative Commons license. The specific license under which this article is published is noted on the first page.

For articles published under [CC BY](#) licenses, you may freely distribute, adapt, or reuse the article, including for commercial purposes, provided you give proper attribution.

For articles published under [CC BY-NC](#) licenses, you may distribute, adapt, or reuse the article for non-commercial purposes. Commercial use requires prior permission from the American Association for the Advancement of Science (AAAS). You may request permission by clicking [here](#).

The following resources related to this article are available online at <http://advances.sciencemag.org>. (This information is current as of March 31, 2017):

Updated information and services, including high-resolution figures, can be found in the online version of this article at:

<http://advances.sciencemag.org/content/1/11/e1500501.full>

Supporting Online Material can be found at:

<http://advances.sciencemag.org/content/suppl/2015/12/08/1.11.e1500501.DC1>

This article **cites 64 articles**, 12 of which you can access for free at:

<http://advances.sciencemag.org/content/1/11/e1500501#BIBL>

Science Advances (ISSN 2375-2548) publishes new articles weekly. The journal is published by the American Association for the Advancement of Science (AAAS), 1200 New York Avenue NW, Washington, DC 20005. Copyright is held by the Authors unless stated otherwise. AAAS is the exclusive licensee. The title *Science Advances* is a registered trademark of AAAS